Desalination and Water Treatment
www.deswater.com

doi: 10.5004/dwt.2018.21965

108 (2018) 65–75
March

Simulation of small-scale thermal water desalination using biomass energy

Ali Amiri[a], Aiman Al-Rawajfeh[b], Catherine E. Brewer[a,*]

[a]*Department of Chemical & Materials Engineering, New Mexico State University, Las Cruces, NM 88003, USA, Tel. +1 (575) 646 8637; Fax: +1 (575)646 7706, emails: cbrewer@nmsu.edu (C.E. Brewer), amiri@nmsu.edu (A. Amiri)*
[b]*Department of Chemical Engineering, Tafila Technical University, P.O. Box 179, 66110 Tafila, Jordan, Tel. +96 232250412; email: aimanr@yahoo.com*

Received 29 May 2017; Accepted 28 January 2018

ABSTRACT

Thermal desalination of brackish groundwater is one way to obtain fresh water from available water sources in rural areas. Some desalination systems use energy sources readily available in rural areas: sunlight, wind, and geothermal. One energy resource that is available but has not been much explored for desalination is biomass. In this study, a hypothetical interface to connect biomass pyrolysis and thermal water desalination was modeled. The initial desalination unit consisted of a two-effect multiple effect distillation unit capable of producing 42 kg/h of fresh water. The model results indicated that approximately 183 kg dry biomass/m^3 distillate is needed and the produced water cost is 318 ± 8 USD/m^3 distillate. Increasing the number of effects and modifying the operating conditions resulted in a scenario where the distillate cost could be reduced to approximately 20 USD/m^3, indicating some potential for this kind of renewable energy–powered desalination system.

Keywords: Multiple effect distillation; Biomass; Biochar; Pyrolysis; Thermal desalination

1. Introduction

Water quality is categorized as a function of the water's total dissolved solids (TDS) content in parts per million (ppm = mg/L): fresh water contains 200–700 ppm, treated wastewater contains 700 to 1,500 ppm, brackish water contains 2,000–10,000 ppm and seawater contains 30,000–60,000 ppm. Depending on the TDS of the water, treatment costs, and infrastructure availability, a variety of desalination techniques can be used; these techniques are grouped into membrane processes, such as reverse osmosis (RO), and thermal processes, such as multiple-effect distillation (MED) and multi-stage flash [1–5]. Some advantages of thermal desalination processes over membrane desalination processes are higher product water quality (i.e. lower TDS of the product water), no membrane replacement costs (i.e. lower maintenance costs), complete boron and arsenic removal, lower carbon footprint if powered by low-grade waste heat [5,6], lower sensitivity to changes in feedwater quality, and less rigid monitoring requirements [7–10]. Membrane maintenance associated with RO systems, in addition to membrane costs and availability, may be a difficulty, especially for non-expert operators in rural communities [11]. MED is the most mature thermal desalination process and has a typical plant capacity of 600–300,000 m^3/d. MED is composed of several evaporation units or "effects" that reuse the water's heat of vaporization [12,13].

The total capacity of installed desalination plants around the world was 200,000 m^3/d in 1966, 23,000,000 m^3/d in 1998, 38,000,000 m^3/d in 2004, and about 80,000,000 m^3/d in 2013 [14,15]. There is a growing body of literature that recognizes the importance of using renewable and smaller-scale energy sources to power desalination systems, especially for remote areas and rural communities where electricity supply or generation is difficult or prohibitively expensive at the necessary scale [7,16,17]. Some desalination systems are designed to use renewable energy sources available in these areas: solar [1,18–21], wind [1,22–25], and geothermal

* Corresponding author.

[1,26–28]. Such systems have been employed with some success. However, significant capital costs for renewable energy systems result in higher fresh water costs compared with existing conventional energy systems. Operation at the small-scale also increases per unit fresh water costs compared with conventional large-scale units. For example, a typical solar membrane distillation unit with a capacity of 0.5–10 m^3/d consumes 540–708 MJ/m^3, resulting in a fresh water cost of 10.50–19.50 USD/m^3 [16]. The fresh water cost for a solar MED system with a capacity of 1 m^3/d is about 25.30 USD/m^3 [22]. The U.S. Bureau of Reclamation and the California Department of Water Resources, for example, operated a thermal desalination demonstration project, Sephton VTE, at the Salton Sea, in southern California, with a desalination capacity of 190 m^3/d. The Sephton VTE plant operates with the waste heat from an adjacent geothermal power plant owned by CalEnergy Operating Corporation [5]. A small-scale solar water desalination unit developed by Begrambekov et al. [29] was able to produce 2.5 m^3/d of fresh water based on an MED concept. In some countries, such as Saudi Arabia, small-scale photovoltaic RO plants with capacities of 3.2 m^3/d have been employed since 1981 [14]. Robinson et al. [30] constructed and tested a small-scale wind-powered RO system with a capacity of 0.5–1 m^3/d, which was enough for a small, remote community in Australia.

One energy resource available in rural areas that has not been much explored for desalination is biomass. The types of biomass available vary widely by region; in the southwestern U.S. biomass sources include agricultural residues such as cotton gin trash [31], pecan orchard prunings and shells [32], dairy manure [33], and yard waste [34]. The low energy density of biomass dictates that biomass employed for energy production should be used within a few kilometers of its source, which suggests that biomass-powered desalination systems should be on the scale of a single farm, household or commercial operation, of a small grouping of farms or residences [35]. Although combustion and gasification can be used to convert biomass to thermal energy, slow pyrolysis has the added advantage of producing a value-added biochar co-product. This biochar can be used as an adsorbent for additional water treatment, or as a soil amendment to improve soil water use efficiency and fertility [36–39].

The primary aim of this study was to explore the feasibility of using slow pyrolysis of biomass waste to provide the thermal energy needed for a small-scale MED unit to desalinate brackish groundwater; southern New Mexico was the location used to design the initial scenario. The choice of small-scale (less than 1,000 m^3/d) was chosen to locate desalination facilities close to the point of use to lower transportation costs and to make the desalination plants easier to adapt to individual site requirements and existing hydraulic structures [40]. The model development process started with a very small (0.34 m^3/d) two-effect unit that might be used in a laboratory setting for water chemistry research and was expanded to include more realistic size and operating conditions to estimate costs.

2. Methodology

The design process began with the heating steam flow rate of 23 kg/h, based on previously studied ranges for small-scale MED [41], resulting in 42 kg/h of fresh water. The heat transfer medium was later changed to hot water to avoid the handling challenges for sub-atmospheric pressure steam. A 35% water recovery ratio was selected based on the feedwater chemistry using Visual MINTEQ V.3.1 (KTH, Sweden); 35% represents the recovery ratio at which $CaSO_4$ and $CaCO_3$ scaling is minimal at groundwater chemistries relevant to New Mexico. At that recovery ratio and desired water production rate, 120 kg/h of brackish feedwater is required. All of the energy needed for steady-state water desalination came from biomass, with some start-up energy coming from propane, diesel, or electricity. Combustion of the pyrolysis vapors was chosen to ensure that the only products are fresh water, brine, biochar, and carbon dioxide.

Chemical process optimization software, Aspen Plus® V8.8, (from AspenTech, Bedford, MI) was used to model the pyrolyzer–MED interface unit operations based on the thermal energy needs of the MED unit. The model included three continuous, steady-state unit operations: a furnace to combust the non-condensable gases (NCG) and vapors from slow pyrolysis to produce hot flue gas, a shell and tube heat exchanger (HX; heater) to produce hot water using the flue gas heat, and a second shell and tube HX to preheat the feedwater using the hot water. The complete process flow diagram, as well as the stream results, is shown in Fig. 1.

Simulations were first carried out as individual blocks using the results from the other blocks. Once input and output streams neared convergence on an individual block basis, the unit operation blocks were combined into one single process block, and the simulation repeated until convergence was achieved with 0.0001 of tolerance.

2.1. Process flow

The process consists of the following steps:

1. Biomass is converted into chars, bio-oil (as vapors and aerosols), and NCG through partial combustion of the biomass in an auger slow pyrolysis unit.
2. Chars enter a char collection container where some of the cooled flue gases are warmed before being recycled into the pyrolysis unit.
3. Bio-oil vapors, aerosols, and NCG flow into a furnace where they are burned with additional air (from a blower fan) to form carbon dioxide and water;
4. A pump pressurizes heat transfer water to feed into the heater where heat from the combustion furnace warms the water to 73°C.
5. Brackish feedwater is preheated using the condenser unit of the MED, followed by a HX (preheater) connected to the hot heat transfer water stream exiting the heater.
6. Hot heat transfer water exiting the preheater is then fed into the tube side of the first effect to provide heat for feedwater evaporation, before being recycled to the heater at ~60°C.
7. Preheated brackish feedwater is sprayed into the MED's effects in a parallel feed arrangement, creating a falling film over the horizontal heat transfer tubes and producing low-pressure steam that flows into the next effect(s) to provide heat for feedwater evaporation.
8. Brine collected at the bottom of each effect flows into a brine storage tank.

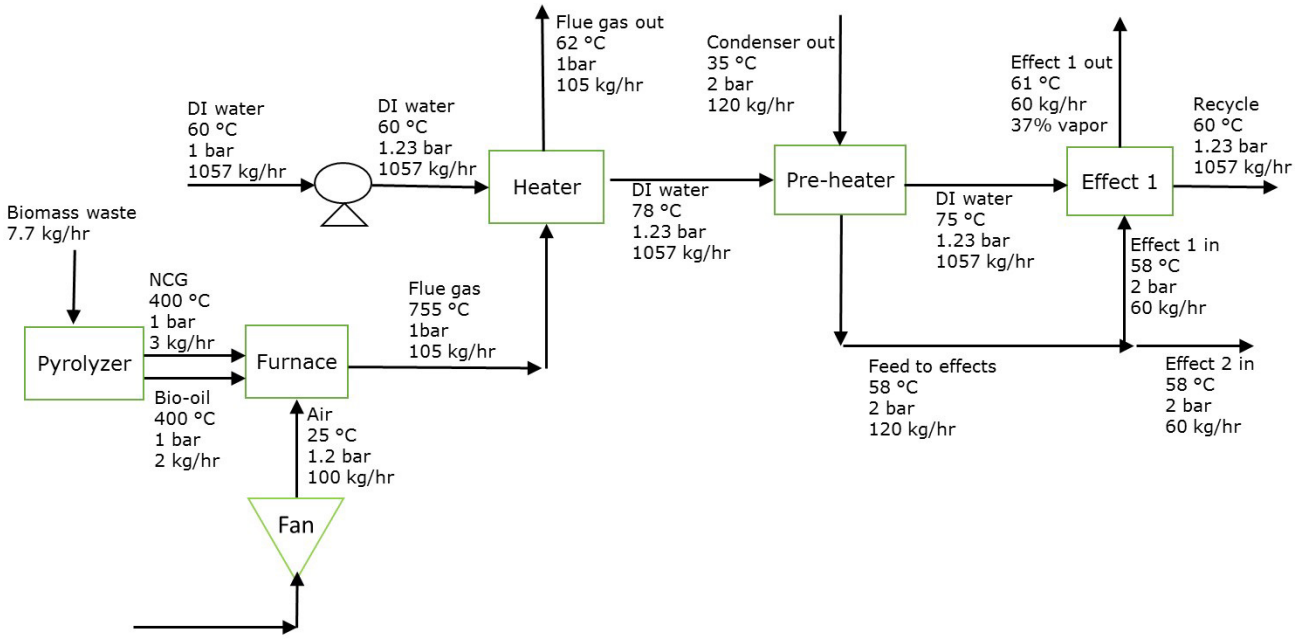

Fig. 1. Aspen Plus® process flow diagram for pyrolyzer–MED interface with stream results.

9. Fresh water collected in the condenser is pumped through a valve into fresh water storage (the sensor and valve allow the diversion of the produced water into the feedwater tank for re-treatment if the electrical conductivity is too high).

2.2. Steam for the MED and thermal energy consumption

To determine the flow rate of fresh water, the performance ratio (PR), defined as the flow rate of distillate produced per flow rate of the primary heat exchange fluid (usually steam), was calculated. PR is closely correlated with the number of effects in MED [42,43]. Delyannis et al. [43] developed a correlation for calculating the PR:

$$\mathrm{PR} = \frac{K\left(1-K^{N}\right)}{1-K} \tag{1}$$

where K is the efficiency of each effect and N is the total number of evaporation units. The average efficiency of each evaporation unit is between 0.85 and 0.95 [43]. Using N = 2 and K = 0.95 (the lowest number of effects and the highest efficiency), respectively, results in a PR of 1.85. If 23 kg/h of primary steam at 81°C, which provides about 14.73 kW of latent heat, is used, the amount of produced fresh water is the target 42 kg/h. Hence, the thermal energy consumption of the MED unit would be 1,260 MJ/m^3.

Here, the heat needed for the MED is provided by the sensible heat of hot water rather than steam due to the difficulty associated with handling low-pressure steam at such a small scale. Based on the heat transfer water temperatures of 75°C and 63°C for the inlet and outlet, respectively, the flow rate of heat transfer water needs to be 1,057 kg/h, to provide 14.73 kW of thermal energy to 60 kg/h of brackish water (TDS = 1,000-5,000 ppm) fed into the two effects [41,44,45]. The maximum temperature drop for the heat transfer water is dictated by the top brine temperature (TBT), such that the difference between the outlet temperature of the heat transfer water (63°C) and the TBT, or temperature approach, is usually 1.5°C–3°C. A temperature approach of 2°C [46,47] and a temperature drop of 2°C across each effect [6] were considered in this study.

Fig. 2 shows the process flow diagram for the parallel/cross flow MED unit. Some advantages of parallel feed (PF) configuration over other configurations, such as forward feed (FF), include less complexity, fewer control connections, fewer number of pumps, no need for a significant heat transfer area in the first effect, and ease of use of chemicals due to similar concentrations in the effects [42,48]. Georgiou and Bonanos [49] also showed that PR in a PF configuration is higher than that of an FF configuration.

The following simplifying assumptions were made in the energy and mass balance calculations: constant specific heat capacity for the distillate, brine, and feedwater; steady-state operation; negligible boiling point elevation; same temperature difference across each effect; salt-free distillate; and no heat loss to the environment [41,47]. The amount of feedwater that can be vaporized in the first effect, M_{s1}, based on a TBT of 61°C and 14.7 kW of thermal energy transfer, is 22.2 kg/h as calculated below [50,51]:

$$M_{s1} = \frac{\left(53{,}038\,\frac{\mathrm{kJ}}{\mathrm{h}} - 60\,\frac{\mathrm{kJ}}{\mathrm{kg}} \times 4.179\,\frac{\mathrm{kJ}}{\mathrm{kg.°C}} \times \left(61-58°\mathrm{C}\right)\right)}{2356\,\frac{\mathrm{kJ}}{\mathrm{kg}}} \tag{2}$$

Produced steam condenses as it heats more feedwater within the second effect. Similarly, steam produced within the second effect through boiling and flash vaporization

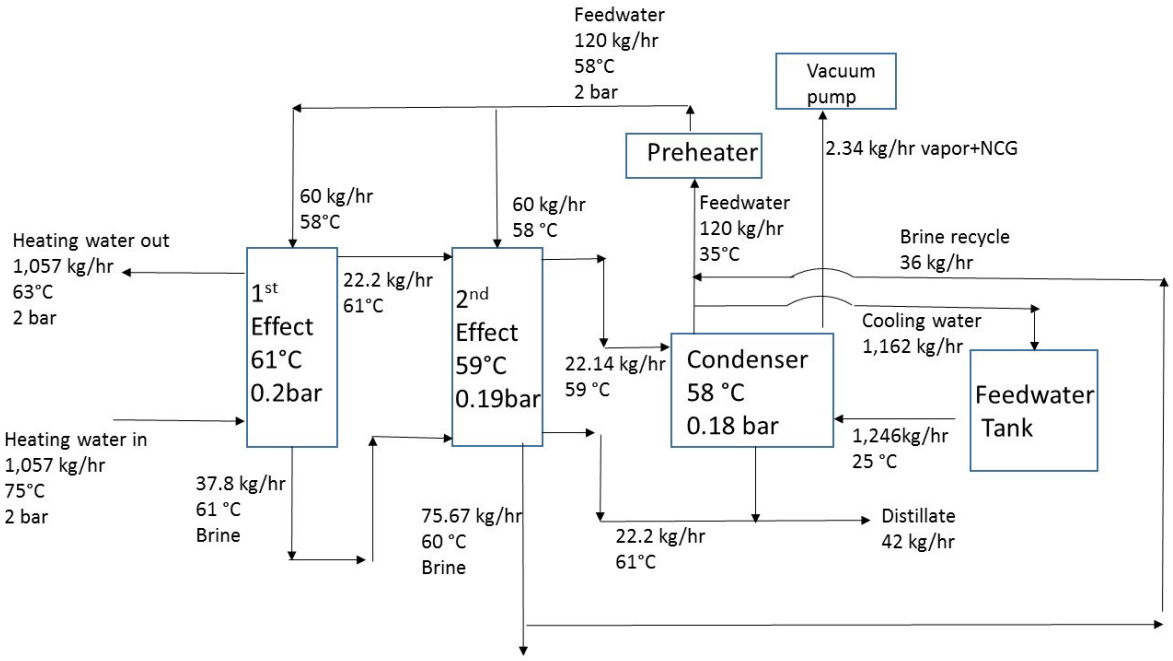

Fig. 2. Process flow diagram of the two-effect parallel-flow MED.

(22.14 kg/h) condenses within the condenser. The condensed steam from the second effect and the condenser constitute the produced distillate. A portion of the steam is lost to the vacuum pump/ejector; recovery could be increased by installing a cold trap.

2.3. Electricity for the MED

Some electrical energy is needed for the biomass pyrolyzer–MED system to operate pumps for movement of the various liquid streams, a blower fan for the furnace, and a vacuum pump to maintain the sub-atmospheric pressures in the effects. The total electrical power requirement is calculated as 365 W, or 31.3 MJ/m^3 (8.7 kWh/m^3) of produced fresh water. Details of electrical energy consumption for each component of the model are included in the supplementary material. Beside their high electrical energy consumption and relatively high maintenance requirements, a noteworthy limitation of vacuum pumps is their low steam tolerance. The role of the vacuum pump is to remove NCG, such as O_2 and CO_2, which are released in the effects during evaporation or through ambient air leakage. The NCG, which usually accumulate around the condenser tubes, decrease the heat transfer coefficient due to their low thermal conductivity, reduce the condensing temperature, and promote corrosion reactions [42].

2.4. Simulation block assumptions

2.4.1. Heater

A countercurrent shell and tube HX heats 1,057 kg/h of warm deionized water to 78°C for heat transfer. The hot (flue gas) side of the heater was modeled using PENG ROBINSON vapor only; the cold (water) side was modeled using STEAM-NBS liquid only. The minimum approach temperature was set to 1°C.

2.4.2. Preheater

To prevent temperature drop within the MED effects, the feedwater should enter the effect at a temperature as close to the saturation temperature as possible. A countercurrent shell and tube exchanger preheats the brackish feedwater from 35°C to 58°C. Both the hot and cold sides of the preheater were modeled using STEAM-NBS liquid only.

2.4.3. Effect 1

A countercurrent shell and tube HX was used to model the first effect. The hot side (heat transfer water) was modeled using STEAM-NBS liquid only, and the cold side (brackish feedwater) was modeled using STEAM-NBS vapor and liquid.

2.4.4. Furnace

In the furnace block, the NCG and bio-oil compositions and combustion reactions were modeled using eight combustion reactions using Peng Robinson property models:

$$CH_4 + 2O_2 \rightarrow CO_2 + 2H_2O$$

$$2H_2 + O_2 \rightarrow 2H_2O$$

$$2CO + O_2 \rightarrow 2CO_2$$

$$C_6H_5OH\ (\text{phenol}) + 7O_2 \rightarrow 6CO_2 + 3H_2O$$

$$CH_3COOH + 2O_2 \rightarrow 2CO_2 + 2H_2O$$

$$C_5H_4O_2\ (\text{furfural}) + 5O_2 \rightarrow 5CO_2 + 2H_2O$$

$$2C_3H_6O_2\ (\text{acetol}) + 7O_2 \rightarrow 6CO_2 + 6H_2O$$

$$2C_3H_6O_2\ (\text{methyl acetate}) + 7O_2 \rightarrow 6CO_2 + 6H_2O$$

The mole fractions for the NCG input stream were 68% CO_2, 28% CO, 2% H_2, and 2% CH_4, at a temperature of 400°C and atmospheric pressure [39,52]. The bio-oil input stream was set at 400°C and atmospheric pressure with mole fractions of 53% phenol, 28.1% acetic acid, 9.2% furfural, 5.4% methyl acetate, and 4.3% hydroxyacetone (acetol) [39,53]. The pressurized air assumed 20% excess air, and an input temperature, pressure, and flow rate of 25°C, 1.2 bar, and 100 kg/h, respectively. The furnace efficiency was assumed to be 80%, based on a standard gas-fueled boiler. Furnace operation was optimized by varying the air flow rate and combustion temperature. Input flow rates were adjusted as different heat duties were modeled.

3. Results

3.1. Simulation results

Fig. 1 shows the unit operations, mass flow rates, temperatures, pressures, and duties for the complete pyrolyzer–MED system with two effects. For a 100 kg/h flow rate of air into the furnace, the simulation converged for a minimum of 2 kg/h NCG and 3 kg/h bio-oil. The net heat duty for the furnace was 5,773 W. The heat duty and heat transfer areas for heater and pre-heater were 22,139 W and 0.22 m^2, and 3,483 W and 0.15 m^2, respectively.

3.2. Calculation of biomass needs

To calculate the amount of biomass needed per cubic meter of produced water, the combined mass flow rates from the bio-oil and NCG streams (5 kg/h) were divided by the pyrolysis yields on a dry basis. Since bio-oil and NCG yields for slow pyrolysis are usually 60%–70%, a 65% yield was used here.

$$M_{db}\text{to produce } 42\,kg/\text{h of distillate} = \frac{\frac{5\text{kg}}{\text{h}}}{0.65} = 7.7\ kg/h \tag{3}$$

$$M_{db}/m^3\text{of distillate} = \frac{7.7\,\frac{\text{kg biomass}}{\text{h}}}{42\,\frac{\text{kg fresh water}}{\text{h}}} \times \frac{1\text{kg water}}{1\text{L}} \times \frac{1\text{L}}{0.001\text{m}^3} = 183\ kg\ \text{biomass}/m^3 \tag{4}$$

The total amount of biomass required, therefore, is 7.7 kg/h, or 183 kg dry biomass per m^3 of produced distillate.

3.3. Cost analysis

Preliminary economic calculations for the interface unit operations, pyrolyzer, and the MED unit are divided into capital costs and operating costs [54].

3.3.1. Capital costs

Total capital costs (CAPEX) included direct costs, indirect costs (IC), contingency, and working capital (WC). Direct costs included the total purchased equipment costs (TPEC) and total installed equipment costs (TIEC). Indirect costs included engineering expenses, and legal and contractor's fees. Contingency represented unexpected expenses such as weather-related delays or construction errors. The TPEC estimated here was $8,440: $5,900 for all interface equipment including furnace, fan, heater, pre-heater, and a pump; $1,500 for a slow pyrolyzer with 7.7 kg/h capacity [54,55]; $400 for a vacuum pump; $300 for the brine and distillate pumps; and $340 for a small-scale MED unit with 0.34 m^3/d production capacity based on 8 h/d. The MED price is a rough estimation based on the CAPEX for industrial scale MED; the economy of scale is not taken into account [56]. TIEC, which includes the full cost of purchased and installed equipment, was estimated as 225% of TPEC, or $18,990. IC, contingency, and WC were calculated at $6,750, $5,150, and $4,630, respectively. Hence, total CAPEX or total project investment (TPI) was $35,520 [54].

3.3.2. Operating costs

Operating costs (OPEX) included direct costs and IC as well as capital charges. The direct, or variable costs, included raw materials, co-product credits, unit operation labor, utilities, and maintenance and repairs. The indirect, or fixed costs, included overhead, taxes, and insurance [54]. OPEX calculations assumed a capacity factor of approximately 1/3 (~8 h/d averaged over the entire year). Raw material purchase costs were set at $0 for the baseline, assuming biomass was abundantly available on-site. Co-product credits assumed the biochars produced by the slow pyrolysis reaction could be sold locally for 500 USD/ton (per the U.S. Biochar Initiative), resulting in a total co-product credit of 3,900 USD/year [57]. Labor was estimated at 21,900 USD/year based on the minimum wage in NM. Maintenance and repair costs ranged from 600 to 3,090 USD/year based on 2%-10% of the fixed capital investment (FCI), which includes the sum of indirect capital costs, TIEC, and contingency. The utility costs include the cost of the 365 W electricity for 8 h/d for 120 USD/year based on average price of the electricity in the United States ($0.12/kWh) [58]. Indirect operating costs included overhead, such as fringe benefits and unemployment insurance, local taxes, and insurance. Overhead costs were estimated at 50%–70% of the sum of labor and maintenance. Local taxes assumed 1%–2%, and insurance costs assumed 0.4%-1.0% of FCI. Overhead, local taxes, and insurance were calculated to be 12,500-17,500 USD/year; 300-620 USD/year; and 120-300 USD/year, respectively [54]. Annual finance charges assumed a loan which was used to purchase the equipment and that payment would be 5%–20% of the TPI. Assuming an interest rate of 10% and payment period of 20 year, the finance charges would be 12% of the TPI or 4,200 USD/year based on the following equation [54,59]:

$$\text{Finance Charges} = \frac{\text{TPI} \times i \times (1+i)^n}{(1+i)^n - 1} \tag{5}$$

The assumed costs resulted in an OPEX of 38,400–47,600 USD/year or 34,500-43,700 USD/year with

the sale of biochar. On a produced water basis, therefore, OPEX would be 280-350 USD/m^3.

Fig. 3 shows that the most substantial portion in CAPEX is TPEC; significant OPEX are labor, overhead, and capital charges.

3.4. Reducing distillate cost by increasing number of evaporator units

The number of the effects is limited by the temperature difference between the heat transfer fluid and the brackish water inlet temperature [6]. The number of effects can be increased by either increasing the TBT or by decreasing the temperature of the last effect from 58°C to <51°C by providing more vacuum. Increasing the TBT 61°C to 80°C–100°C for this kind of brackish water chemistry would likely need nanofiltration or forward osmosis pretreatment to reduce the concentration of scale-forming ions [60–62].

Tables 1 and 2 compare the increase in OPEX and CAPEX from the addition of more evaporators (effects) to the MED unit. As more effects are added to increase the number of times the latent heat of evaporation is reused, CAPEX increases faster than OPEX. Among all expenses, the labor cost is the largest. To simplify the comparison, biochar sales are not included in Tables 1 and 2.

Adding more effects to the MED results in more distillate per unit of energy in the heat transfer fluid and reduces the fresh water cost. Fig. 4 presents the minimum selling price

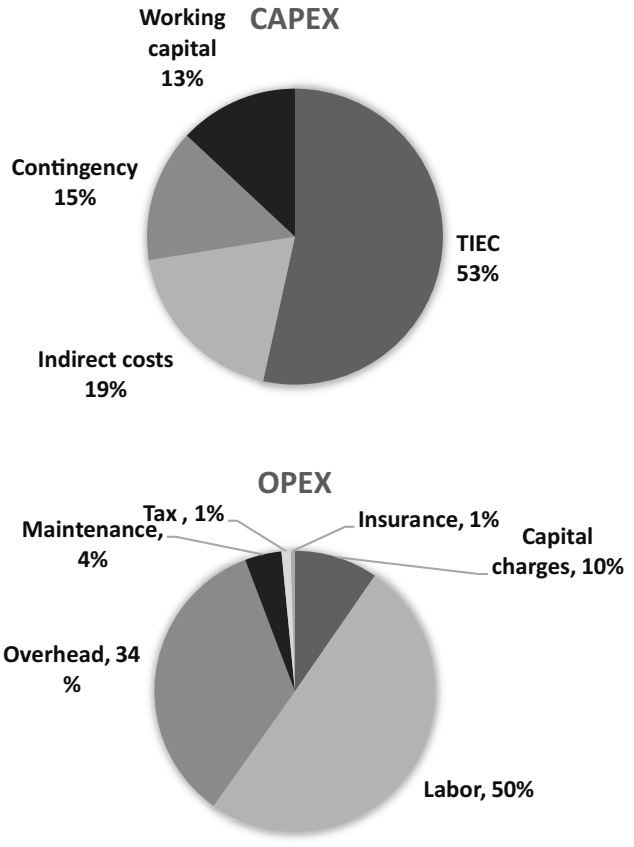

Fig. 3. Proportions of each cost within CAPEX and OPEX for a two-effect MED unit, pyrolyzer, and interface components.

(MSP) for the distillate as the number of effects is increased. MSP is the lowest product cost (market price) for which the net present value is zero after a specified period. MSP can be given by the equation as follows [54].

$$\mathrm{NPV} = \sum \frac{\text{Market price}\left(\frac{\mathrm{USD}}{\mathrm{m}^3}\right) \times \text{yield}\left(\frac{\mathrm{m}^3}{\mathrm{y}}\right) - (\mathrm{OPEX} + \mathrm{TPEC})}{(1+i)^n} \tag{6}$$

where n is the lifetime of the facility, i is a predetermined discount rate, and yield is the production capacity. Here, the facility lifetime and discount rate were set to 20 years and 10%, respectively [54].

3.5. Statistical analysis

A statistical analysis of the produced water cost was conducted assuming normal distribution using the univariate procedure in SAS® (from SAS Institute, Cary, NC). Average OPEX and produced water cost, with biochar sales, for the two-effect MED were 39,100 USD/year with a standard deviation of 1,020 USD/year and 318 USD/m^3 with a standard deviation of 8.3 USD/m^3, respectively. The values for the optimum four-effect MED were 39,400 USD/year with a standard deviation of 1,033 USD/year and 166 USD/m^3 with a standard deviation of 4.4 USD/m^3. The produced water costs for the two-effect and four-effect MED units, without biochar sales, were 349 and 183 USD/m^3, respectively. Fig. 5 illustrates the kernel density estimation of the water cost for the four-effect MED. Kernel distribution is a nonparametric representation of the probability density function of water costs. The skewness of the graph was 0.019, toward the high-cost side.

3.6. Reducing distillate cost by increasing heat transfer fluid flow rate

Using a higher heat transfer fluid flow rate can reduce specific energy consumption and distillate cost by increasing heat transfer rates [63]. Fig. 6 shows the effect of increasing the heat transfer water flow rate for the two-effect MED

Table 1
Changes in CAPEX as the number of effects in the MED unit increases from 2 to 10

	WC	Contingency	IC	TIEC
2 Effects	4,634	5,148	6,752	18,990
3 Effects	4,723	5,248	6,882	19,356
4 Effects	4,808	5,342	7,006	19,706
5 Effects	4,888	5,431	7,123	20,034
6 Effects	4,959	5,510	7,227	20,327
7 Effects	5,034	5,594	7,337	20,634
8 Effects	5,103	5,670	7,437	20,917
9 Effects	5,165	5,739	7,527	21,170
10 Effects	5,229	5,810	7,621	21,432

Note: All units are USD

Table 2.
Changes in OPEX as the number of effects in the MED unit increases from 2 to 10

	Insurance	Tax	Maintenance	Overhead	Labor	Capital charges
2 Effects	216	463	1,853	14,252	21,900	4,263
3 Effects	220	472	1,889	14,273	21,900	4,345
4 Effects	224	480	1,923	14,294	21,900	4,423
5 Effects	228	488	1,955	14,313	21,900	4,497
6 Effects	231	495	1,983	14,330	21,900	4,562
7 Effects	234	503	2,013	14,348	21,900	4,632
8 Effects	238	510	2,041	14,365	21,900	4,695
9 Effects	241	516	2,066	14,380	21,900	4,752
10 Effects	244	522	2,091	14,395	21,900	4,811

Note: All units are USD/year.

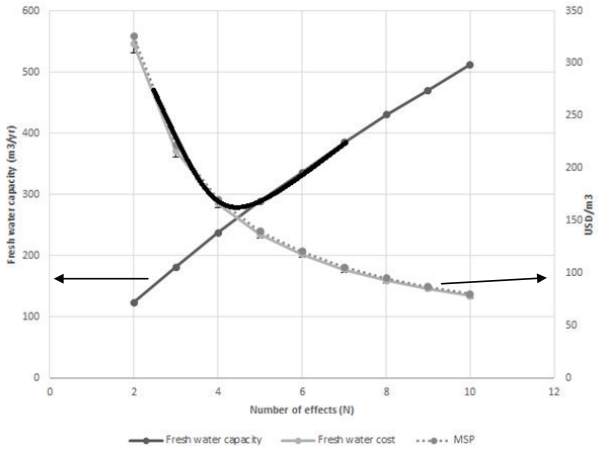

Fig. 4. Impact of number of effects on distillate production capacity, distillate cost, and minimum selling price (MSP) over 20 years.

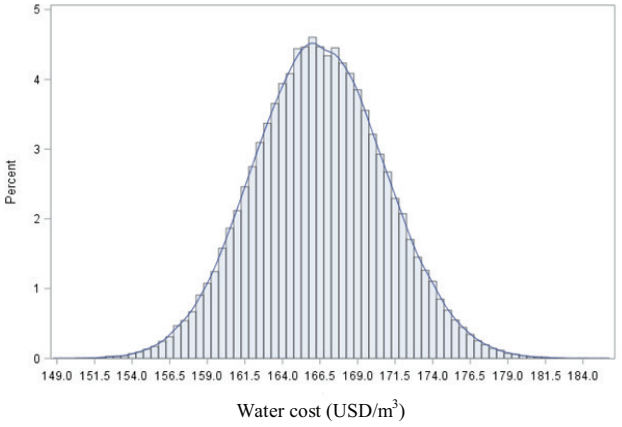

Fig. 5. Kernel density curve of fresh water cost based on the four-effect MED unit with the pyrolyzer and interface components.

unit, assuming 10% increase in TPEC as flow rate increased from 1,057 kg/h up to 22,984 kg/h, equivalent to a heating steam flow rate of 500 kg/h. The TPEC increase for the MED unit was estimated using reported costs for industrial scale MED systems [56]. As Fig. 6 shows, increasing the heating water flow rate to 22,984 kg/h reduces the estimated distillate cost for a 2-effect, 4-effect, and 10-effect MED to 19, 11, and 6 USD/m^3, respectively. For the heating water flow rate of 9,193 and 22,984 kg/h, the specific energy consumption decreases to 0.99 and 0.39 kWh/m^3, respectively.

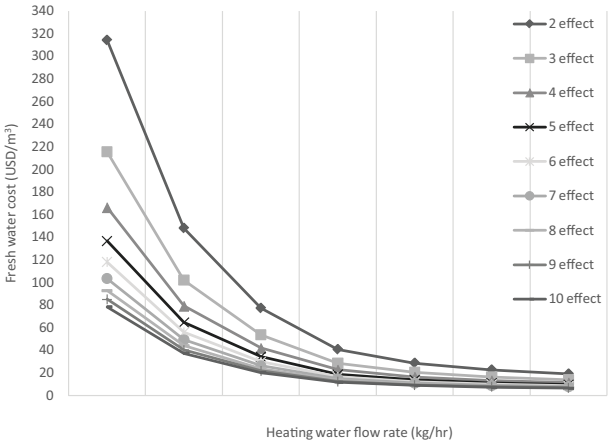

Fig. 6. Impact of increasing heating water flow rate on distillate cost for MED units with different numbers of effects.

4. Discussion

4.1. MED compared with RO for brackish water desalination

Even though thermal desalination is energy and capital intensive, several reports have shown the advantages of thermal desalination over membrane technologies, especially for low-temperature MED when low-grade heat from geothermal energy or process waste heat is available [6,47,51,64,65]. If a biomass pyrolysis–RO system was to be used instead of a biomass pyrolysis–MED system, a micro-scale (<15 kW) biomass combined heat and power (CHP) system would be the best option. Development of such CHP systems is still in the early stages, and their applications are restricted by several economic and technical barriers [66–68]. A 35 kW biomass CHP unit using updraft gasification of biomass with a

heating value of 19 MJ/kg, has an electrical efficiency of 18% (6% more than using direct combustion) and would have an installed specific cost of 7,140 Euro/kWe (approximately 9,500 USD/kWe in 2010) [69].

A typical brackish water RO unit, with an energy recovery system and a production rate of up to 98,000 m^3/d, consumes about 5.4–9 MJ/m^3 (1.5–2.5 kWh/m^3) of electrical energy [4,70]. A typical single-purpose MED unit, with a capacity of 5,000–15,000 m^3/d, and 12–20 effects, requires 145–230 MJ/m^3 of thermal energy and 8.1 MJ/m^3 (2.25 kWh/m^3) of electrical energy [16,71]. The reasons for the higher specific energy consumption of the MED unit modeled here, compared with a typical industrial unit, include using a vacuum pump rather than a steam/water ejector and low distillate production rate. The electrical energy consumption of the MED system could reduce to 1.5 kWh/m^3 if an ejector was used to supply the vacuum rather than a vacuum pump. At such a small scale, ejectors would have to be custom-designed [47,72].

In this study, MED was chosen because of two aspects of water chemistry that can affect RO efficiency for brackish water in this region: As(III) and B. For an RO membrane to remove As(III), upstream chlorination is needed to convert As(III) to As(V). Since chlorine oxidizes conventional membranes, removal of residual chlorine is required upstream of the RO membrane. Boron content in the brackish water in southern New Mexico, USA, exceeds 0.5 ppm, the standard limit defined by the World Health Organization for drinking water. Boron removal requires multiple RO stages at high pH (>10). The low boron removal of brackish water membranes (15%–20%), the higher water recovery used in brackish water RO compared with seawater RO, and the chance of alkaline scaling decrease the feasibility of adding a second RO pass at high pH. A boron-specific ion-exchange system, therefore, would be needed if a two-stage RO system was used on this type of brackish water [59,73–75].

4.2. Brine disposal

Brine disposal for inland desalination systems is a challenging issue. Evaporation ponds are usually the least expensive brine disposal method, especially for arid and semi-arid areas where the evaporation rate is high [74,76]. Constantly changing regulations may affect the applicability of evaporation ponds. Due to the small brine flow rate for this system and the high evaporation rate in the southwestern United States, use of a small evaporation pond with this system is an appropriate solution. Clay or synthetic membrane liners, such as PVC, can be used underneath the pond to prevent contamination of the underlying potable water aquifers [76,77].

4.3. Water blending

The TDS of the distillate from MED is less than 5 ppm, which may be substantially purer than applications require. For boiler applications, however, the distillate would be used without any blending. If the distillate were used for irrigation, the distillate could be blended with untreated water up to 175 ppm for sensitive crops such as vegetables, 350 ppm for field crops, and 960 ppm for forage crops [78]. If the distillate were used for human drinking water, the distillate could be blended up to a maximum of 500 ppm. Such blending could decrease the overall water costs slightly.

4.4. Biochar sales

Biochar may have a selling price from 200 to 2,000 USD/ton of biochar, depending on its quality and demand [57,79]. Increased biochar sales can reduce the fresh water cost. Over 20 years, increasing the biochar sales price to 2,000 USD/ton (15,800 USD/year) based on the heating water flow rate of 1,057 kg/h, decreases the distillate cost for two-effect and four-effect MED to 229 and 116 USD/m^3, respectively [57].

5. Conclusions

This study was undertaken to design an interface to connect a biomass slow pyrolyzer to a very small-scale MED unit that could produce fresh water using residual biomass energy. For a two-effect MED unit, 7.7 kg/h of dry biomass is needed to produce 42 kg/h of distillate, which converts to 183 kg biomass/m^3 distillate. Techno-economic analysis calculations indicate that using 1,057 kg/h of heat transfer water with a two-effect and four-effect MED results in a fresh water cost of 318 ± 8.3 and 166 ± 4.4 USD/m^3, respectively. The distillate cost for two-effect and four-effect MED can reduce to 19 and 11 USD/m^3 (comparable costs with other small-scale renewable energy-powered MED systems) by increasing the equipment size and using a 22,984 kg/h heat transfer fluid flow rate.

Acknowledgments

This work is supported by a cooperative agreement between New Mexico State University and the U.S. Bureau of Reclamation. The authors would like to acknowledge the NMSU Manufacturing Engineering & Technology Center for their assistance with fabricating the lab-scale pyrolyzer and the MED. They also wish to acknowledge Dr. Kyriacos Zygourakis for his input on the interface design, Dr. Mary Billiot for her input on managerial accounting, Mr. Jose Peña, Mr. Michael Smith, and Mr. Willian Do Prado for their assistance with MED experiments, and Mr. Hamed Doshmanfana for his assistance with brackish water analysis.

Symbols

C_p	—	Heat capacity, J/kg.°C
HX	—	Heat exchanger
IC	—	Indirect costs
M	—	Mass flow rate, kg/h
MED	—	Multiple effect distillation
n	—	Number of effects
NCG	—	Non-condensable gases
NPV	—	Net present value
OPEX	—	Operating costs
PR	—	Performance ratio
Q	—	Heat transfer, W
RO	—	Reverse osmosis
ΔT	—	Temperature difference, °C
Ts	—	Saturation temperature, °C
TBT	—	Top brine temperature, °C
TDS	—	Total dissolved solids, ppm
TIEC	—	Total installed equipment costs
TPEC	—	Total purchased equipment costs

TPI	—	Total project investment
WC	—	Working capital
db	—	Dry basis

References

[1] S.A. Kalogirou, Seawater desalination using renewable energy sources, Prog. Energy Combust., 31 (2005) 242–281.
[2] D.S. Likhachev, F.-C. Li, Large-scale water desalination methods: a review and new perspectives, Desal. Wat. Treat., 51 (2013) 2836–2849.
[3] R.G. Raluy, L. Serra, J. Uche, Life cycle assessment of desalination technologies integrated with renewable energies, Desalination, 183 (2005) 81–93.
[4] R. Semiat, D. Hasson, Water desalination, Rev. Chem. Eng., 28 (2012) 43–60.
[5] J. Tonner, Barriers to Thermal Desalination in the United States, Bureau of Reclamation, Denver, CO, 2008.
[6] A. Ophir, F. Lokiec, Advanced MED process for most economical sea water desalination, Desalination, 182 (2005) 187–198.
[7] M.A. Eltawil, Z. Zhengming, L. Yuan, A review of renewable energy technologies integrated with desalination systems, Renew. Sust. Energy Rev., 13 (2009) 2245–2262.
[8] A. Hanson, W. Zachritz, K. Stevens, L. Mimbela, R. Polka, L. Cisneros, Distillate water quality of a single-basin solar still: laboratory and field studies, Sol. Energy, 76 (2004) 635–645.
[9] S. Kalogirou, Survey of solar desalination systems and system selection, Energy, 22 (1997) 69–81.
[10] B.A. Stewart, R. Lal, Advances in Soil Science, Springer-Verlag New York Inc., New York, NY, 1985.
[11] L. Kelley, H. Elasaad, S. Dubowsky, Autonomous operation and maintenance of small-scale PVRO systems for remote communities, Desal. Wat. Treat., 55 (2015) 1–13.
[12] H.T. El-Dessouky, H.M. Ettouney, Multiple-effect evaporation desalination systems. thermal analysis, Desalination, 125 (1999) 259–276.
[13] H.T. El-Dessouky, H.M. Ettouney, F. Mandani, Performance of parallel feed multiple effect evaporation system for seawater desalination, Appl. Thermal Eng., 20 (2000) 1679–1706.
[14] C.C.K. Liu, Wind-Powered Reverse Osmosis Water Desalination for Pacific Islands and Remote Coastal Communities, Bureau of Reclamation, Denver, CO, 2009.
[15] A.D. Khawaji, I.K. Kutubkhanah, J.-M. Wie, Advances in seawater desalination technologies, Desalination, 221 (2008) 47–69.
[16] A. Al-Karaghouli, L.L. Kazmerski, Energy consumption and water production cost of conventional and renewable-energy-powered desalination processes, Renew. Sust. Energy Rev., 24 (2013) 343–356.
[17] L. Garcia-Rodriguez, Renewable energy applications in desalination: state of the art, Solar Energy, 75 (2003) 381–393.
[18] L. García-Rodríguez, C. Gómez-Camacho, Perspectives of solar-assisted seawater distillation, Desalination, 136 (2001) 213–218.
[19] L. García-Rodríguez, A.I. Palmero-Marrero, C. Gómez-Camacho, Application of direct steam generation into a solar parabolic trough collector to multieffect distillation, Desalination, 125 (1999) 139–145.
[20] L. García-Rodríguez, A.I. Palmero-Marrero, C. Gómez-Camacho, Comparison of solar thermal technologies for applications in seawater desalination, Desalination, 142 (2002) 135–142.
[21] V.G. Gude, N. Nirmalakhandan, S. Deng, Desalination using solar energy: towards sustainability, Energy, 36 (2011) 78–85.
[22] A. Al-Karaghouli, D. Renne, L.L. Kazmerski, Solar and wind opportunities for water desalination in the Arab regions, Renew. Sust. Energy Rev., 13 (2009) 2397–2407.
[23] C.T. Kiranoudis, N.G. Voros, Z.B. Maroulis, Wind energy exploitation for reverse osmosis desalination plants, Desalination, 109 (1997) 195–209.
[24] M.S. Miranda, D. Infield, A wind-powered seawater reverse-osmosis system without batteries, Desalination, 153 (2003) 9–16.
[25] Q. Ma, H. Lu, Wind energy technologies integrated with desalination systems: review and state-of-the-art, Desalination, 277 (2011) 274–280.
[26] A. Ophir, Desalination plant using low grade geothermal heat, Desalination, 40 (1982) 125–132.
[27] L. Awerbuch, T.E. Lindemuth, S.C. May, A.N. Rogers, Geothermal energy recovery process, Desalination, 19 (1976) 325–336.
[28] K. Bourouni, R. Martin, L. Tadrist, Analysis of heat transfer and evaporation in geothermal desalination units, Desalination, 122 (1999) 301–313.
[29] L. Begrambekov, A. Gordeev, S. Vergasov, A. Zakharov, Desalination device for arid areas, Desal. Wat. Treat., 31 (2011) 387–391.
[30] R. Robinson, G. Ho, K. Mathew, Development of a reliable low-cost reverse osmosis desalination unit for remote communities, Desalination, 86 (1992) 9–26.
[31] A. Isci, G.N. Demirer, Biogas production potential from cotton wastes, Renew. Energy, 32 (2007) 750–757.
[32] J.M. Lillywhite, R. Heerema, J.E. Simonsen, E. Herrera, Pecan Marketing Channels in New Mexico, Guide Z-307, New Mexico State University Cooperative Extension Service, Las Cruces, NM, 2010.
[33] X. Cao, W. Harris, Properties of dairy-manure-derived biochar pertinent to its potential use in remediation, Bioresour. Technol., 101 (2010) 5222–5228.
[34] D.R. Hill, A.A. Jennings, Bioasphalt from Urban Yard Waste Carbonization: A Student Study, Ohio Department of Transportation, 2011.
[35] M. Wright, R.C. Brown, Establishing the optimal sizes of different kinds of biorefineries, Biofuels Bioprod. Biorefin., 1 (2007) 191–200.
[36] J. Lehmann, J. Pereira da Silva, C. Steiner, T. Nehls, W. Zech, B. Glaser, Nutrient availability and leaching in an archaeological Anthrosol and a Ferralsol of the Central Amazon basin: fertilizer, manure and charcoal amendments, Plant Soil, 249 (2003) 343–357.
[37] R. Lal, Black and buried carbons' impact on soil quality and ecosystem services, Soil Till. Res., 99 (2008) 1–3.
[38] Y. Lee, P.-R.-B. Eum, C. Ryu, Y.-K. Park, J.-H. Jung, S. Hyun, Characteristics of biochar produced from slow pyrolysis of Geodae-Uksae 1, Bioresour. Technol., 130 (2013) 345–350.
[39] A.N. Phan, C. Ryu, V.N. Sharifi, J. Swithenbank, Characterisation of slow pyrolysis products from segregated wastes for energy production, J. Anal. Appl. Pyrol., 81 (2008) 65–71.
[40] J. Martinez Beltran, S. Koo-Oshima, Water Desalination for Agricultural Applications, Food and Agriculture Organization of United Nations, Rome, 2004.
[41] P.K. Sen, P.V. Sen, A. Mudgal, S.N. Singh, S.K. Vyas, P. Davies, A small scale multiple-effect distillation (MED) unit for rural micro enterprises: part I--design and fabrication, Desalination, 279 (2011) 15–26.
[42] H.T. El-Dessouky, H.M. Ettouney, Fundamentals of Salt Water Desalination, Elsevier, Amsterdam, 2002.
[43] A.A. Delyannis, E.A. Delyannis, Sauerstoff: Anhangband Water Desalting Wasser-Entsalzung, Springer-Verlag Berlin, 2013.
[44] H. El-Dessouky, I. Alatiqi, S. Bingulac, H. Ettouney, Steady-state analysis of the multiple effect evaporation desalination process, Chem. Eng. Technol., 21 (1998) 437–451.
[45] I.S. Al –Mutaz, A.A. Al- Mojjly, M.E. Abashar, Thermal and Brine Dispersion from Coastal MSF Desalination Plants, King Saud University, Saudi Arabia.
[46] A. Christ, K. Regenauer-Lieb, H.T. Chua, Thermodynamic optimisation of multi effect distillation driven by sensible heat sources, Desalination, 336 (2014) 160–167.
[47] B. Rahimi, A. Christ, K. Regenauer-Lieb, H.T. Chua, A novel process for low grade heat driven desalination, Desalination, 351 (2014) 202–212.
[48] M.A. Darwish, H.K. Abdulrahim, Feed water arrangements in a multi-effect desalting system, Desalination, 228 (2008) 30–54.
[49] M.C. Georgiou, A.M. Bonanos, A transient model for forward and parallel feed MED, Desal. Wat. Treat., 57 (2016) 23119–23131.

[50] P. Palenzuela, D. Alarcón, G. Zaragoza, J. Blanco, M. Ibarra, Parametric equations for the variables of a steady-state model of a multi-effect desalination plant, Desal. Wat. Treat., 51 (2013) 1229–1241.
[51] A. Christ, X. Wang, K. Regenauer-Lieb, H.T. Chua, Low-grade waste heat desalination technology, Int. J. Simul. Multidiscip. Design Optim., 7 (2014) 1–6.
[52] W. Wijayantia, K.I. Tanoue, Char formation and gas products of woody biomass pyrolysis, Energy Procedia, 32 (2013) 145–152.
[53] K.H. Kim, X. Bai, M. Rover, R.C. Brown, The effect of low-concentration oxygen in sweep gas during pyrolysis of red oak using a fluidized bed reactor, Fuel, 124 (2014) 49–56.
[54] R.C. Brown, T.R. Brown, Biorenewable Resources, Wiley Blackwell, Ames, IA, 2014.
[55] T.R. Brown, M.M. Wright, R.C. Brown, Estimating profitability of two biochar production scenarios: slow pyrolysis vs fast pyrolysis, Biofuels Bioprod. Biorefin., 5 (2011) 54–68.
[56] N.M. Wade, Distillation plant development and cost update, Desalination, 136 (2001) 3–12.
[57] N. Kulyk, Cost-Benefit Analysis of the Biochar Application in the U.S. Cereal Crop Cultivation, University of Massachusetts-Amherst, 2012.
[58] State Electricity Profiles, U.S. Department of Energy, 2016. Available at: http://www.eia.gov/electricity/state/.
[59] S. Loutatidou, H.A. Arafat, Techno-economic analysis of MED and RO desalination powered by low-enthalpy geothermal energy, Desalination, 365 (2015) 277–292.
[60] A.E. Al-Rawajfeh, S. Ihm, H. Varshney, A.N. Mabrouk, Scale formation model for high top brine temperature multi-stage flash (MSF) desalination plants, Desalination, 350 (2014) 53–60.
[61] A. Altaee, A. Mabrouk, K. Bourouni, P. Palenzuela, Forward osmosis pretreatment of seawater to thermal desalination: high temperature FO-MSF/MED hybrid system, Desalination, 339 (2014) 18–25.
[62] C. Sommariva, Thermal Desalination Processes and Economics, International Desalination Association, 2017. Available at: https://ocw.mit.edu/courses/mechanical-engineering/2-500-desalination-and-water-purification-spring-2009/readings/MIT2_500s09_lec18.pdf.
[63] L. Yang, S. Shen, H. Hu, Thermodynamic performance of a low temperature multi-effect distillation experimental unit with horizontal-tube falling film evaporation, Desal. Wat. Treat., 33 (2011) 202–208.
[64] X. Wang, A. Christ, K. Regenauer-Lieb, K. Hooman, H.T. Chua, Low grade heat driven multi-effect distillation technology, Int. J. Heat Mass Transfer, 54 (2011) 5497–5503.
[65] H. Shih, Evaluating the technologies of thermal desalination using low-grade heat, Desalination, 182 (2005) 461–469.
[66] H. Liu, G. Qiu, Y. Shao, F. Daminabo, S.B. Riffat, Preliminary experimental investigations of a biomass-fired micro-scale CHP with organic Rankine cycle, Int. J. Low Carbon Technol., 5 (2010) 81–87.
[67] G. Pei, J. Li, Y. Li, D. Wang, J. Ji, Construction and dynamic test of a small-scale organic rankine cycle, Energy, 36 (2011) 3215–3223.
[68] L. Dong, H. Liu, S. Riffat, Development of small-scale and micro-scale biomass-fuelled CHP systems – a literature review, Appl. Thermal Eng., 29 (2009) 2119–2126.
[69] S.R. Wood, P.N. Rowley, A techno-economic analysis of small-scale, biomass-fuelled combined heat and power for community housing, Biomass Bioenergy, 35 (2011) 3849–3858.
[70] S.A. Avlonitis, K. Kouroumbas, N. Vlachakis, Energy consumption and membrane replacement cost for seawater RO desalination plants, Desalination, 157 (2003) 151–158.
[71] R. Semiat, Energy issues in desalination processes, Environ. Sci. Technol., 42 (2008) 8193–8201.
[72] H. El-Dessouky, H. Ettouney, I. Alatiqi, G. Al-Nuwaibit, Evaluation of steam jet ejectors, Chem. Eng. Process., 41 (2002) 551–561.
[73] E.H. Ezechi, M.H. Isa, S.R.B.M. Kutty, Boron in produced water: challenges and improvements: a comprehensive review, J. Appl. Sci., 12 (2012) 402.
[74] L.F. Greenlee, D.F. Lawler, B.D. Freeman, B. Marrot, P. Moulin, Reverse osmosis desalination: water sources, technology, and today's challenges, Water Res., 43 (2009) 2317–2348.
[75] P. Glueckstern, M. Priel, Boron removal in brackish water desalination systems, Desalination, 205 (2007) 178–184.
[76] M. Ahmed, W.H. Shayya, D. Hoey, A. Mahendran, R. Morris, J. Al-Handaly, Use of evaporation ponds for brine disposal in desalination plants, Desalination, 130 (2000) 155–168.
[77] L. Katzir, Y. Volkmann, N. Daltrophe, E. Korngold, R. Mesalem, Y. Oren, J. Gilron, WAIV - Wind aided intensified evaporation for brine volume reduction and generating mineral byproducts, Desal. Wat. Treat., 13 (2010) 63–73.
[78] G. Fipps, Irrigation Water Quality Standards and Salinity Management Strategies, Texas A&M AgriLife Extension, 2013.
[79] S. Shabangu, D. Woolf, E.M. Fisher, L.T. Angenent, J. Lehmann, Techno-economic assessment of biomass slow pyrolysis into different biochar and methanol concepts, Fuel, 117 (2014) 742–748.

Supplementary material

Electrical energy consumption

The power requirements for the pumps were calculated according to the equation below [1]:

$$\text{Pumping power}\left(\text{kW}\right)=\frac{\rho\left(\frac{\text{kg}}{\text{m}^3}\right).g\left(\frac{\text{m}}{\text{s}^2}\right).h\left(\text{m}\right).Q(\frac{\text{m}^3}{\text{s}})}{\eta_{\text{pump}}.\eta_{\text{motor}}} \quad (1)$$

η_{pump} and η_{motor} which are the pump and motor efficiency were assumed to be 0.7 and 0.9, respectively, in this study.

Assuming PVC tubing and negligible minor friction loss, the power requirement for the pumps were as follows:

- 10.5 W for the hot water pump for a 20 ft (6.1 m) length, 2 m hydraulic head, 3/4 in (1.9 cm) hose diameter, 1,057 kg/h flow rate, and 0.34 m friction loss [2],
- 12.4 W for the feedwater pump for a 20 ft (6.1 m) length, 2 m hydraulic head, 3/4 in (1.9 cm) hose diameter, 1,246 kg/h flow rate, and 0.34 m friction loss [2],
- 6.7 and 3.7 W for the brine and distillate pump, respectively, based on 2 bar differential pressure for pumping from vacuum to the atmospheric pressure [1].
- 32 W for a blower to provide air to the pyrolysis vapor combustion chamber at 100 kg/h.
- 300 W for a vacuum pump to maintain system pressure at approximately 0.2 bar (20 kPa absolute) assuming a rotary piston pump and a fluid (air) flow rate of 1.5–2 kg/h [3]. This pressure corresponds to a water vapor saturation temperature of approximately 60°C.

References

[1] B. Rahimi, A. Christ, K. Regenauer-Lieb, H.T. Chua, A novel process for low grade heat driven desalination, Desalination, 351 (2014) 202–212.
[2] Friction Loss Table, Hunter Industries, 2016. Available at: https://www.hunterindustries.com/sites/default/files/tech_friction_loss_charts.pdf.
[3] IPS, Engineering Standard for Process Design of Vacuum Equipment, Iranian Petroleum Standards, 1993.